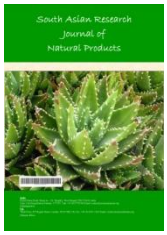

South Asian Research Journal of Natural Products

5(1): 29-42, 2022; Article no.SARJNP.88254

Magnetic Field Dependent Thermosolutal Convection Flow between Two Squeezing Plates

Muhammad Basit Ali Khan [a], Rehan Ali Shah [a*] and Sohail Khan [b]

[a] Department of Basic Science and Islamiat, University of Engineering and Technology, Peshawar, Pakistan.
[b] Department of Basic Science and Islamiat, Jiangsu University China, Peshawar, Pakistan.

Authors' contributions

This work was carried out in collaboration among all authors. All authors read and approved the final manuscript.

Article Information

Open Peer Review History:
This journal follows the Advanced Open Peer Review policy. Identity of the Reviewers, Editor(s) and additional Reviewers, peer review comments, different versions of the manuscript, comments of the editors, etc are available here: https://www.sdiarticle5.com/review-history/88254

Original Research Article

Received 06 April 2022
Accepted 11 June 2022
Published 30 June 2022

ABSTRACT

The effect of magnetic field dependent thermosolutal convection and MFD viscosity of the fluid dynamic are studied between two squeezing plates. The unsteady constitutive expression of mass conservation modified naiver-stocks, Maxwell and MFD thermosolutal convection are coupled as a system of ordinary differential equations. The corresponding solution for momentum as well as solution for the magnetic field equations are determined by the PCM method. The validity and accuracy of PCM results is proved by the comparison of the PCM solution with numerical solver package BVP4c.It has been shown the magnetic Reynold number caused to decrease the flow, magnetic field distribution and temperature of the fluid. Also x-component and y- component of magnetic field have opposite behavior with increase in MFD viscosity.

Keywords: Thermosolutal convection; reynold number; cartesian coordinate; magnetic field.

NOMENCLATURE

p	Pressure	C	Dimensional Concentration
x, y, z	Cartesian coordinate	$\varkappa$	Thermal Conductivity
U_x	x-Component of Velocity($m.s^{-1}$)	μ	Dynamic Viscosity
U_y	y-Component of Velocity($m.s^{-1}$)	ν	Kinematic Viscosity

**Corresponding author: Email: rehanshah@uetpeshawar.edu.pk;*

U_z	z-Component of Velocity($m.s^{-1}$)	σ	Electrical Conductivity
t	Time(s)	ρ	Fluid Density
T_u	Temperature at Upper Plate(k)	α	Positive Constant
T_l	Temperature at Lower Plate(k)	η	Similarity Variable
C_u	Concentration at Upper Plate	θ	Dimensionless Variable
C_l	Concentration at Lower Plate	φ	Dimensionless Variable
p_r	Prandtl Number(υ/k)	$'$	Derivative w.r.t η
N_b	Squeezing Parameter	$*$	Dimensionless Variable
D(t)	Distance between Two Plates	u	Fluid Condition on Upper Plate
c_p	Specific Heat of Fluid($^{j}/_{kgk}$)	l	Fluid Condition on Upper Plate
H_m	Hartmann Number	U	Fluid Velocity($m.s^{-1}$)
E_c	Eckert Number	T	Fluid Temperature
m_η	Magnetic Field Dependent Viscosity	P_m	Pyro Magnetic Coefficient
N_{em}	Magnetic Reynold Number	P_s	Salinity Magnetic Coefficient
N_C	Strength of Magnetic Field		

1. INTRODUCTION

Research based studies show that magnetic fields can reduce the heart attack risk by streamlining the blood flow. Tao and Huang showed that when magnetic field is applied parallel to blood direction, it significantly reduced blood viscosity. This processes widely used in engineering (fluid film in power transmission, hydro magnetic lubrication of breaking devices and pistons system in engines). Ferro hydrodynamics (FHD) is mechanics of fluid motion under magnetic polarization. Magnetic fluids are involved in heat transfer processes via Ferro fluids. Liquid cooled are example of such processes, in which Ferro fluids carry heat away from coils. [1]. This invention increases the coil's amplifying capacity, which contributes to high fidelity sound generation in loud speakers. Another crucial application of magnetic field is in the field of drug designing where magnetic field is used to carry drug to desired target sites in the human body, a drop of Ferro fluid in human body can be detected by the magnetic field [2]. According to Lenz's law when conducting fluid move in magnetic field then magnetic field changes its motion. In MHD, the motion changes the field and vice versa [3,4]. Alloys have important applications in heat transfer processes such a steel, brass and bronze are few typical examples. Alloys have applications in various fields including powder technology, aerospace technology and in surgeries. Recently Aamir et al. [5] studied the Theremosolutal convection between coaxial contracting disc and investigated the fluid dynamic aspects of these magnetic field dependent discs. They studied their problem in cylindrical coordinate system and analyzed the flow field, temperature variation, skin fraction and Nusselt number.

2. LITERATURE REVIEW

The study of squeezing flow has it origin in the 19th century and continues to receive considerable attention due to practical application in physical and biophysical area. Stoke problems of a convective flow past a perpendicular infinite plates in a spinning systems in occurrence of inconsistent magmatic field was studied by Mutua et al. [6]. He concluded that velocity field and temperature depend upon all of the parameters. The effect of these parameters changes the rate of heat transfer as well as the skin friction. It was observed that that increasing magnetic parameter (M) and Eckert number (Ec) elevated the free convection heating and as free convection cooling velocity profile. Seth [7] examined heat transfer and MHD flow on a porous flat plate along with mass transfer. Fluid velocity component was observed to be raised as the Hall parameter and value of time was increased. Unsteady flow between two permeable squeezed plates with thermal radiation has been studied by Victor [8]. For analysis he used Galerkin finite element method. He concluded that the fluid velocity and temperature distribution are strongly depended on Radiation parameter and on Prandle number. In his study he also concluded that Grashof number and Magnetic parameter have a negligible effect on temperature distribution. Inclined magnetic field applied on coutee flow inside two parallel porous plates. was studied by Simon [9]. He considered the lower plate is absorbent and motionless. He found that fluid velocity decrease with a rise in magnetic field. For the solution of the magnetic squeeze film problem Rashidi et al. [10] used the DTM-Pade combined method to determine convergence,

stability and versatility. The important effect of changing the electrical conductivity of a viscous, incompressible and electrically conducting fluid on the free convection flow was observed. Furthermore, it was noted that heat transfer on the isothermal non conducting plate was also influenced by changing the electrical conductivity. Shorma et al. [11] Studied natural convection flow and heat generation in electrically conductivity flow. It was reported that suitable magnetic field can change aerodynamic force along with heat transfer rates in convenient manner. This type of MHD studies are linked with fission reactor development where the plasma is restricted by use of strong magnetic field [12]. MHD effects in the so-called blanket was studied by Morley [13]. The blanket is present between the magnetic field coils and plasma. Blanket is used for the avoiding radiation damages. Sohail et al [14]. explored the way in which flow between two squeezing plates is effecting by changing the magnetic field Recently aamir et al. [15] studied the theremosolutl convection between coaxial contracting disc and investigated the fluid dynamic aspects of these magnetic field dependent discs. They studied their problem is cylindrical coordinate system then analyzed the flow field, temperature variation, skin fraction and nusselt number. Nath and murugesan investigatate[16] the influence of nano particles shape on heat and mass transport phenomena in a moving lid cavity under the combined effect of thermosolutal buoyancy force and magnetic force. The diffusion moved of transport processes is stronger then the convection mode at higher inclination angle of magnetic field.nusselet and Sherwood number respectively except the platelet shape that shows that maximum fractional loss in term of wall shear stress. The dynamical model follows the usual conservation laws and is reduced through a nonsimilar group of transformations. The resulting equations are solved using a spectral-based local linearization method, and the accuracy of the numerical results is validated through the grid dependence and convergence tests. Detailed analyses of the effects of specific thermophysical parameters are presented through tables and graphs. The study reveals, among other results, that the buoyancy force, solute and thermal expansion coefficients, and thermal radiation increase the overall wall drag, heat, and mass fluxes [17] studied by tijani.

2.1 Problems Formulation

Suppose that an incompressible and axisymmetric viscous fluid divided by the distance of $y = l\sqrt{1-\alpha t}$ between two parallel squeezing plates, where l is length equal to the separation of plates at t=0. For α>0 both plates are pressed until they reach at $t = \frac{1}{\alpha}$ both are separated at α< 0 . Lower plate is stationary and upper plate are squeeze it is considered to be the optimal conductor for both surfaces, according to hughes. The electrical forces are much smaller than the magnetic forces and consequently are ignored in the present problem. The applied magnetic field produced to induced magnetic field (B_x, B_y, B_z)

$$H_x = \frac{\alpha x E_0}{(\mu_2(1-\alpha T)} \quad H_y = \frac{-xE_0}{\mu_1 1-\alpha t^{0.5}} \quad H_z = \frac{xF_0}{\mu_2(1-\alpha t)}$$

E_0 and F_0 are dimensionless $\mu_1 and \mu_2$ are the external and inner media magnetic permeability between the two plates , respective ely. Incompressible fluid is presumed to have a variable viscosity given by $\mu = \mu_0(1 + \partial.B)$ in the absence of the magnetic field μ_0 is the viscosity of the fluid. $\partial_x = \partial_y = \partial_z$ isotropic was taken for the variance coefficient of viscosity ∂. The component of the μ are $\mu_x = \mu_0(1 + \partial B_x)$, $\mu_y = \mu_0(1 + \partial B_Y)$ and $\mu_z = \mu_0(1 + \partial B_Z)$ further $B = \mu_p(M + H)$ whear M is magnetization H is magnetic field and μ_p is magnetic permeability. The effect of shear viscosity dependency is not taken into account since it has a marginal effect on a high field mono dispersive device. The equations governing viscous fluid flow and heat transfer are:

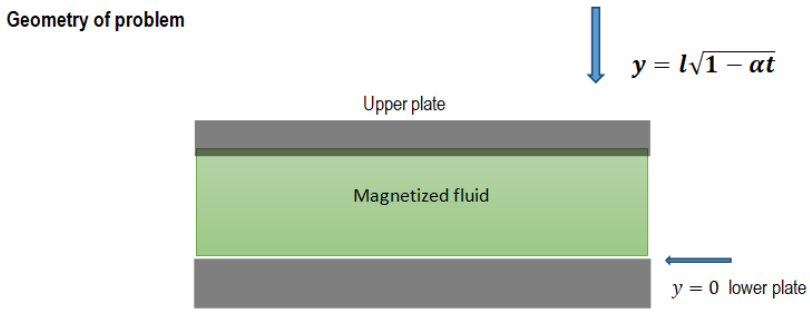

2.2 Basic Governing Equations

Continuity equation

$$\nabla . U = 0 \quad (1)$$

Maxwell equation

$$\nabla . B = 0 , \quad \nabla \times B = 0 \quad (2)$$

Novier stoke equation

$$\rho \left[\frac{\partial U}{\partial t} + (U.\nabla)U\right] + \nabla p - \mu \nabla^2 U - \frac{1}{\mu_2}(\nabla \times B) \times B = 0 \quad (3)$$

Magnetic field equation

$$\frac{\partial B}{\partial t} - \nabla \times (U \times B) - \frac{1}{\sigma \mu_2}\nabla^2 B = 0 \quad (4)$$

Solute concentration equation is

$$[\rho_0 C_{s,h} - \mu_0 H.(\frac{\partial M}{\partial T})]\frac{DT}{Dt} + \mu_0 T(\frac{\partial M}{\partial T})\frac{DH}{Dt} = K_1 \nabla^2 T \quad (5)$$

Solute concentration

$$[\rho_0 C_{s,h} - \mu_0 H.(\frac{\partial M}{\partial C})]\frac{DC}{Dt} + \mu_0 C(\frac{\partial M}{\partial C})\frac{DH}{Dt} = K'_1 \nabla^2 C \quad (6)$$

U is fluid velocity, σ is electrical conductivity, ρ_0 is reference density, ρ is the density of fluid, p is pressure of fluid, μ is variable dynamic viscosity, $C_{s,h}$ is specific heat of constant volume, T is temperature, C is solute concentration, M is magnetization, K_I is thermal conductivity, K'_I solute conductivity.

Boundary condition are chosen as:

$$U_x = 0 \ , U_y = 0, \ U_z = \frac{\sigma_1 x}{1-\alpha t} \ , \quad B_x = 0, \quad B_y = 0 \quad B_z = 0 .$$

$$T = T_l \ , C = C_l \ at \ Y = 0.$$

$$U_x = 0 \, , U_y = \frac{-\alpha l}{2\sqrt{1-\alpha t}} \, , U_z = \frac{\sigma_u x}{1-\alpha t} .$$

$$B_x = 0 \, , B_y = \frac{-xE_0}{\sqrt{1-\alpha t}},$$

$$B_z = \frac{xF_0}{1-\alpha t} .$$

$$T = T_u, \quad C = C_u \ at \ y = l\sqrt{1-\alpha t} . \quad (7)$$

Where U_x, U_y, U_z are respectively the x, y and z component of the velocity, $\alpha, T_l and C_l$ represent the thermal diffusivity temperature at lower plate and concentration at lower plate are respectively, while temperature and concentration at upper plate are represent by T_u, C_u respectively, c_ρ specific heat at constant pressure. Introducing the following similarity transformation are chosen for reducing the partial differential equations (1) to (6) to a system of ordinary differential equations.

$$U_x = \frac{\alpha x}{2(1-\alpha t)} m'(\eta), \qquad U_y = \frac{-\alpha l}{\sqrt{1-\alpha t}} m(\eta) ,$$

$$U_z = \frac{\sigma_l x}{1-at} n(\eta) \ , \qquad B_x = \frac{axE_0}{2L^2(1-at)} h'(\eta) ,$$

$$B_y = \frac{-aE_0}{l\sqrt{1-at}} h(\eta) \qquad , B_z = \frac{2\upsilon x F_0}{al(1-at)} k(\eta)$$

$$\theta = \frac{T-T_u}{T_l - T_u}, \quad \varphi = \frac{C-C_u}{C_l - C_u}, \quad \eta = \frac{y}{l\sqrt{1-at}} \quad . \quad (8)$$

The partial differential equations (3.1) to (3.6) are transform in the form of following ordinary differential equations.

$$m'''' = \frac{N_b}{m_\eta}[2m'' + \eta m''' - 2mm'''' + 2N_C^2 N_{em}\left(2hh' + \eta hh'' + 2h^2 m'' - 2hmh''\right) . \quad (9)$$

$$n'' = \frac{1}{m_\eta}[N_b\left(2n + \eta n' + m'n - 2mn'\right) - N_c N_d\left(h'k - 2hk'\right). \quad (10)$$

$$h'' = N_{em}\left(h + \eta h' + hm' - mh'\right) . \quad (11)$$

$$k'' = N_{em}\left(2k + \eta k' - 2mk'\right) + \frac{N_c N_{em}}{N_d}\left(hn'\right) . \quad (12)$$

$$\theta'' = N_b P_r\left(\eta\theta' - 2m\theta'\right) - P_m \nabla T H_m E_c \left(2(\eta h\theta' - 2mh\theta' + h\theta + \eta h'\theta - 2mh'\theta'\right). \quad (13)$$

$$\varphi'' = N_b P_r\left(\eta\varphi' - 2m\varphi'\right) - P_c \nabla T H_m E_c \left(2(\eta h\varphi' - 2mh\varphi' + h\varphi + \eta h'\varphi - 2mh'\varphi'\right). \quad (14)$$

Boundary condition are reduced to

$$m(0) = 0 \ , m'(0) = 0 \ , \ n(0) = 1, \ \theta(0) = 1, \ \varphi(0) = 1, \ h(0) = 0, \ k(0) = 0 ,$$

$$m(1) = 0.5 \quad , m'(1) = 0 \ , \ n(1) = 1, \ \theta(1) = 0, \ \varphi(1) = 0, \ h(1) = 1, \ k(1) = 1. \tag{15}$$

Where N_b is rotational Reynold number, N_{em} is magnetic Reynold number N_c is strength of magnetic field in y direction N_d strength of magnetic field in z direction , m_η is magnetic field dependent viscosity parameter. $P_r E_c H_m P_m P_s$ are Prandtl number Eckert number Hartman number pyro magnetic coefficient and salinity magnetic coefficient are respectively.

After solving these equations by PCM methods and BVP4C methods we get a different table and graph are

Table 1. Computation for $m(\eta)$, $n(\eta)$, $h(\eta)$, $k(\eta)$, $\theta(\eta)$ with $N_b = 0.1, N_c = 0.2, \ N_d = 0.5, \ P_r = 0.2, H_m = 1, P_m = 0.2, P_s = 1, N_{em} = 0.3, E_c = 2$, S=1, m_η=0.3 and various values of η.

	Numerical results					PCM results				
η	m(η)	$n(\eta)$	$h(\eta)$	$\theta(\eta)$	$\varphi(\eta)$	m(η)	$n(\eta)$	$h(\eta)$	$\theta(\eta)$	$\varphi(\eta)$
.1	0.0143	0.9171	0.9000	0.9063	0.9157	0.0141	0.9170	0.900	0.9066	0.9157
.2	0.0525	0.8411	0.1805	0.8121	0.8308	0.0522	0.8411	0.1805	0.8127	0.8308
.3	0.1087	0.7725	0.2722	0.7170	0.7452	0.1083	0.7724	0.2722	0.7179	0.7452
.4	0.1767	0.7112	0.3659	0.6190	0.6568	0.1762	0.7112	0.3659	0.6198	0.6568
.5	0.2508	0.6575	0.4620	0.5234	0.5705	0.2500	0.6575	0.4620	0.5237	0.5705
.6	0.3247	0.6113	0.5613	0.4241	0.4805	0.3240	0.6112	0.5613	0.4249	0.4805
.7	0.3926	.5725	0.6644	0.3227	0.3881	0.3920	0.5724	0.6644	0.3232	0.3881
.8	0.4485	0.5411	0.7716	0.2186	0.2923	0.4480	0.5410	0.7716	0.2180	0.2923
.9	0.4863	0.5170	0.8834	0.1112	0.1920	0.4860	0.5170	0.8834	0.1119	0.1920

Table 2. Computation for $m''(\eta)$, $-n'(\eta)$, $-h'(\eta)$, $-k'(\eta)$,- $\theta'(\eta)$ with $N_b = 0.2, N_c = 0.1, N_d = 1, P_r = 2, H_m = 1, P_m = 1, P_s = 0.5, N_{em} = 0.5, E_c = 2$, S=1 and various of m_η

	Numerical results			PCM results		
m_η	$m''(0)$	$-n'(0)$	$-\theta'(0)$	$m''(0)$	$-n'(0)$	$-\theta'(0)$
1	3.0232	0.2524	1.1545	3.0172	0.2521	1.1554
2	3.0146	0.1292	1.1545	3.0086	0.1291	1.1554
3	3.0117	0.869	1.1545	3.0057	0.0867	1.1554
4	3.0103	0.0654	1.1545	3.0043	0.0653	1.1554

Table 3. Computation for $m''(\eta)$, $-n'(\eta)$, $-h'(\eta)$, $-k'(\eta)$,- $\theta'(\eta)$ with $N_b = 0.2, N_c = 0.1, N_d = 1, P_r = 2, H_m = 1, P_m = 0.2, P_s = 0.5, E_c = 2, m_\eta = 3$, S=1 and various values of N_{em}.

	Numerical results			PCM results		
N_{em}	$m''(0)$	$-n'(0)$	$-\theta'(0)$	$m''(0)$	$-n'(0)$	$-\theta'(0)$
.5	3.0117	0.0869	1.1545	3.0057	0.0867	1.1554
1	3.0118	0.0863	1.1334	3.0058	0.0863	1.1342
2	3.0118	0.0853	1.1000	3.0058	0.0853	1.1005
3	3.0118	0.0846	1.0751	3.0058	0.0847	1.0756

Table 4. Computation for $m''(\eta)$,$-n'(\eta)$,$-h'(\eta)$,$-k'(\eta)$,- $\theta'(\eta)$ with $N_b = 0.1, N_c = 2, N_d = 1, P_r = 0.2, H_m = 1, P_m = 0.2, P_s = 1, N_{em} = .3, m_\eta = 3$, S=1 and various values of E_c.

	Numerical results			PCM results		
E_c	$m''(0)$	$-n'(0)$	$-\theta'(0)$	$m''(0)$	$-n'(0)$	$-\theta'(0)$
0.1	3.0127	0.1421	1.0015	3.0068	0.1421	1.0015
0.5	3.0127	0.1421	1.0087	3.0068	0.1421	1.0088
1	3.0127	0.1421	1.0176	3.0068	0.1421	1.0178
1.5	3.0127	0.1421	1.0265	3.0068	0.1421	1.0268

Table 5. Shows $n(\eta)$ and $k(\eta)$ with various values of , N_d and constant values of $N_b = 0.1, N_c = 5, N_{em} = 1, P_r = 1, H_m = 10, P_m = 1, P_s = 1, m_\eta = 2, E_c = 0.1$

	Numerical results			PCM results		
Pm	$m''(0)$	$-n'(0)$	$-\theta'(0)$	$m''(0)$	$-n'(0)$	$-\theta'(0)$
0.1	3.0188	0.1241	1.0114	3.0148	0.1249	1.0114
0.5	3.0188	0.1241	1.0684	3.0148	0.1249	1.0688
1	3.0188	0.1241	1.1370	3.0148	0.1249	1.1377
1.5	3.0188	0.1241	1.2023	3.0148	0.1249	1.2029

Table 6. Computation for $m''(\eta)$, $-n'(\eta)$, $-h'(\eta)$, $-k'(\eta)$,- $\theta'(\eta)$ with $N_b = 0.2, N_c = 0.1$, $P_r = 2, H_m = 1, E_C = 2$, m_η=3 P_m=.5, N_{em}=1, S=1 and various values of P_S.

	Numerical results			PCM results		
Ps	$m''(0)$	$-n'(0)$	$-\varphi'(0)$	$m''(0)$	$-n'(0)$	$-\varphi'(0)$
.1	3.0188	0.1241	1.0116	3.0148	0.1249	1.0114
.5	3.0188	0.1241	1.0672	3.0148	0.1249	1.0688
1	3.0188	0.1241	1.1296	3.0148	0.1249	1.1377
1.5	3.0188	0.1241	1.1854	3.0148	0.1249	1.1998

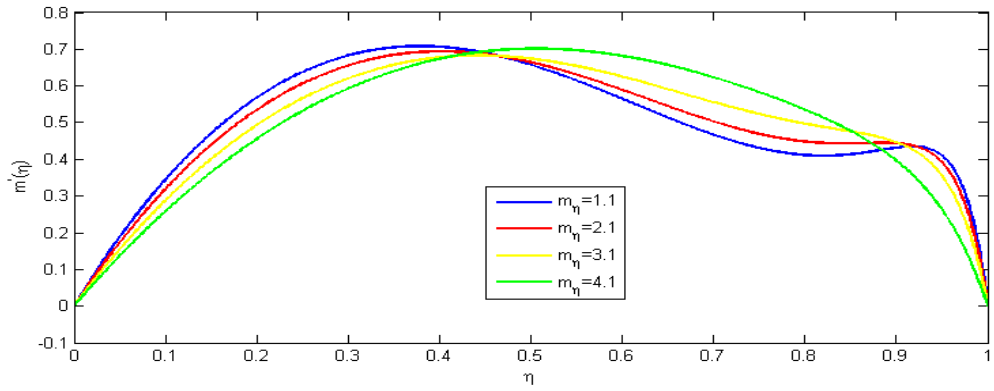

Fig. 1a. Shows the effect of $m'(\eta)$, for various values of m_η and constant values of $N_b = 0.2, N_c = 8, N_d = 1, P_r = 2, H_m = 1, P_m = 9, P_s = 1, N_{em} = 13, E_c = 0.3$

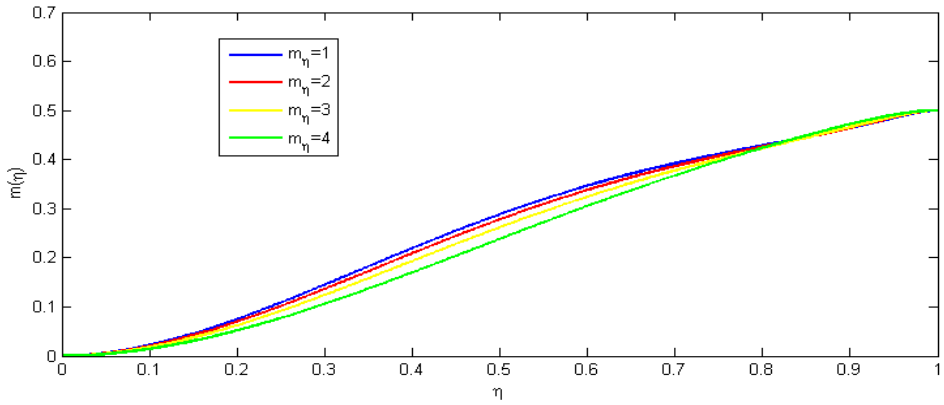

Fig. 1b. Shows the effect of $m(\eta)$, for various values of m_η and constant values of $N_b = 0.2, N_c = 8, N_d = 1, P_r = 2, H_m = 1, P_m = 9, P_s = 1, N_{em} = 13, E_c = 0.3$

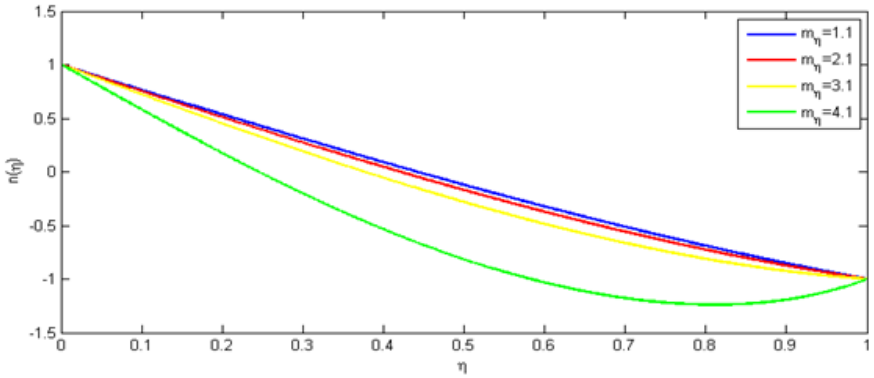

Fig. 2a. Shows the $k(\eta)$ with various values of m_η and constant values of $N_b = .01, N_c = 3, N_d = 2, P_r = .2, H_m = 1, P_m = 1, P_s = .5, N_{em} = 0.5,\ E_c = 0.3$

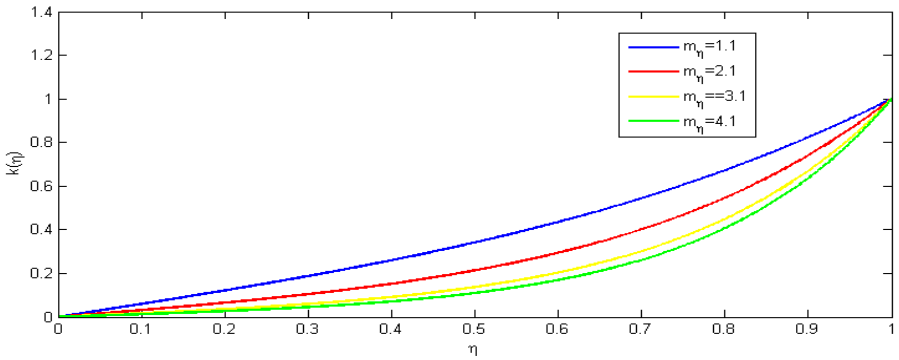

Fig. 2b. Shows the $k(\eta)$ various values of m_η and constant values of $N_b = .01, N_c = 3, N_d = 2, P_r = .2, H_m = 1, P_m = 1, P_s = .5, N_{em} = 0.5,\ E_c = 0.3$

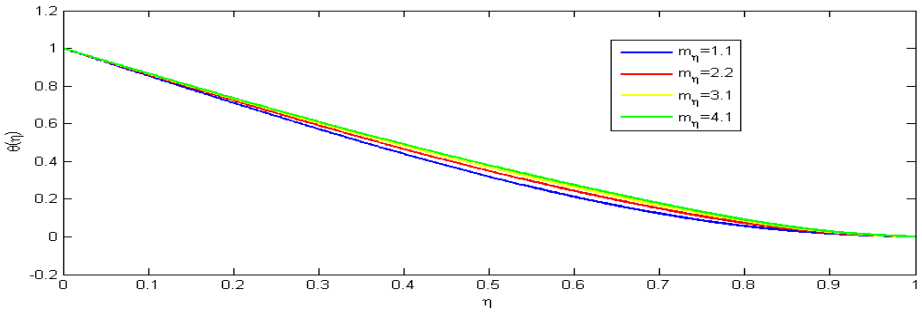

Fig. 2c. Shows the $\theta(\eta)$,various values of m_η and constant values of $N_b = .01, N_c = 3, N_d = 2, P_r = .2, H_m = 1, P_m = 1, P_s = .5, N_{em} = 0.5,\ E_c = 0.3$

3. RESULTS AND DISCUSSION

The effect of MFDV m_η on m(η) and m'(η) can be seen in Fig. 1. The resistance force of fluid flow increases as the viscosity coefficient rises as a result flow velocity deceases. Fig. 1b indicates that as the viscosity of a fluid increases, the fluid flow at the center of the channel decreases that reflect the viscosity function as defined. As the viscosity parameter rises the fluid internal resistance increases as a result the flow decreases. It was also discovered that the fluid flow in the x direction decreases near the lower plate due to inertia and in the central zone it increases and start gradually decrease as it approaches the upper plates. Fig. 2(a) shows the largest reduction in the z-component of velocity n$((\eta))$ near the upper plate for a fixed value of $m_\eta = 4$, while for other various values of m_η, h(η) and k (η) have the opposite behavior.

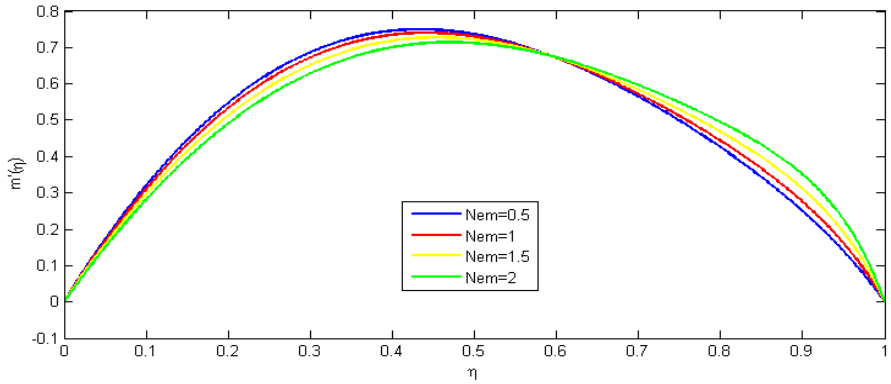

Fig. 3a. Shows the effect of $m'(\eta)$, at the various values of N_{em} and constant values of $N_b = 0.9, N_c = 10, N_d = 0.2, P_r = 0.2, H_m = 1, P_m = 1, P_s = 0.5, m_\eta = 3, E_c = 5$

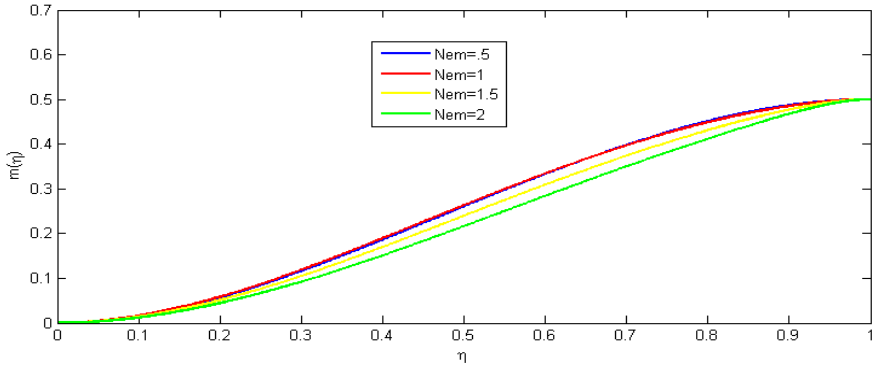

Fig. 3b. Shows the effect of $m(\eta)$ at the various values of N_{em} and constant values of $N_b = 0.9, N_c = 10, N_d = 0.2, P_r = 0.2, H_m = 1, P_m = 1, P_s = 0.5, m_\eta = 3, E_c = 5$

Fig. 3 shows the effect of magnetic Reynold number on velocity component of $m(\eta)$ and $m'(\eta)$ Fig. 3a indicates that as the magnetic Reynold's number increases the velocity component in x-direction decreases in the surrounding of lower plate while it increases near the region of upper plate. This is because the magnetic Reynold number depends upon the squeezing of upper plate as the upper plate moves away from lower plate the ratio of fluid flux to magnetic diffusivity increases and as a result the velocity of fluid increase from central region to upper plate. Similarly opposite behavior can be seen in Fig. 3b where the y-component of velocity increases and its value is maximum is achieved at N_{em} =2 for the specific values of other parameters.

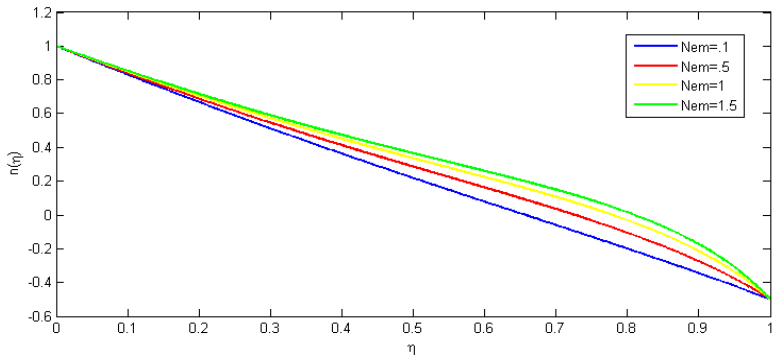

Fig. 4a. shows the effect of $n(\eta)$, with various values 0f N_{em} and at constant values of $N_b = 0.9, N_c = 8, N_d = 0.2, P_r = 0.2, H_m = 10, P_m = 1, P_s = .5, m_\eta = 3, E_c = 5$

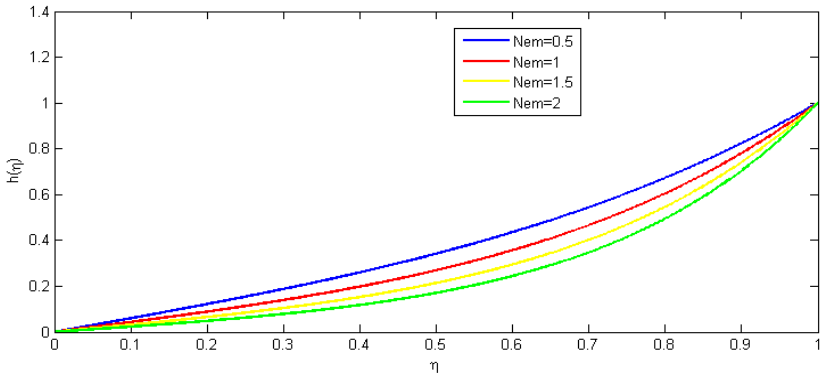

Fig. 4b. shows the effect of $h(\eta)$ with various values 0f N_{em} and at constant values of $N_b = 0.9, N_c = 8, N_d = 0.2, P_r = 0.2, H_m = 10, P_m = 1, P_s = .5, m_\eta = 3, E_c = 5$

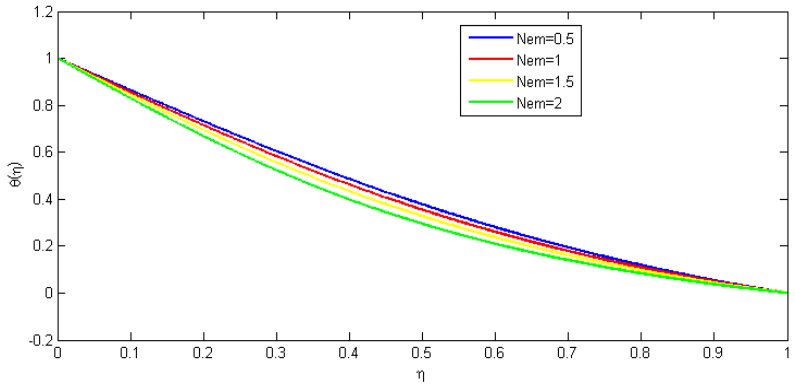

Fig. 4c. shows the effect of $\varphi(\eta)$, with various values 0f N_{em} and at constant values of $N_b = 0.9, N_c = 8, N_d = 0.2, P_r = 0.2, H_m = 10, P_m = 1, P_s = .5, m_\eta = 3, E_c = 5$

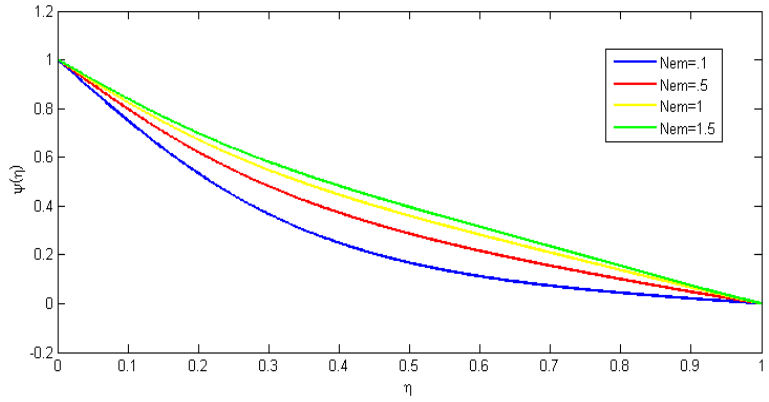

Fig. 4d. Shows the effect $\varphi(\eta)$, with various values 0f N_{em} and at constant values of $N_b = 0.9, N_c = 8, N_d = 0.2, P_r = 0.2, H_m = 10, P_m = 1, P_s = .5, m_\eta = 3, E_c = 5$

Fig. 4a show the effect of magnetic Reynold number on z-component of velocity. From this figure one can observe that on increasing the magnetic Reynold number the z-component of velocity rises. It also observed that on increasing magnetic flux or decreasing diffusivity $h(\eta)$, $\theta(\eta)$ and $\varphi(\eta)$ shows same behavior as shown in Fig. 4(b-d) and clear increases are observed in $\theta(\eta)$ and $\varphi(\eta)$.

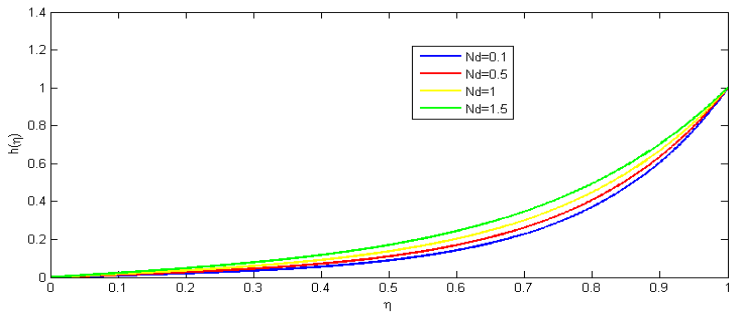

Fig. 5a. Shows $h(\eta)$ and $k(\eta)$ with various values of , N_d and constant values of $N_b = 0.1, N_c = 5, N_{em} = 1, P_r = 1, H_m = 10, P_m = 1, P_s = 1, m_\eta = 2, E_c = 0.1$

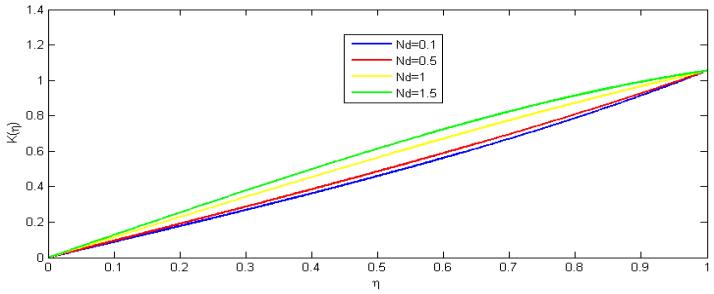

Fig. 5b. Shows $h(\eta)$ and $k(\eta)$ with various values of , N_d and constant values of $N_b = 0.1, N_c = 5, N_{em} = 1, P_r = 1, H_m = 10, P_m = 1, P_s = 1, m_\eta = 2, E_c = 0.1$

Fig. 5 shows the effect of N_d on magnetic component in y-direction i.e. $h(\eta)$ a nd on magnetic component in z-direction i.e. $k(\eta)$. As N_d shows the strength of applied magnetic field along the z axis, so on increasing N_d the magnetic field in z-direction increases.

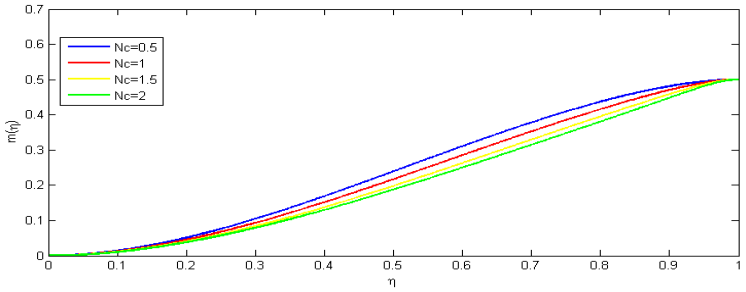

Fig. 6a. Shows the graph of $m'(\eta), m(\eta), n(\eta)$ and $k(\eta)$ with various values of , N_c and constant values of $N_b = 0.1, N_d = .5, N_{em} = 3, P_r = .1, H_m = 10, P_m = 1, P_s = 1, m_\eta = .1, E_c = 0.1,\ N_c = 3$

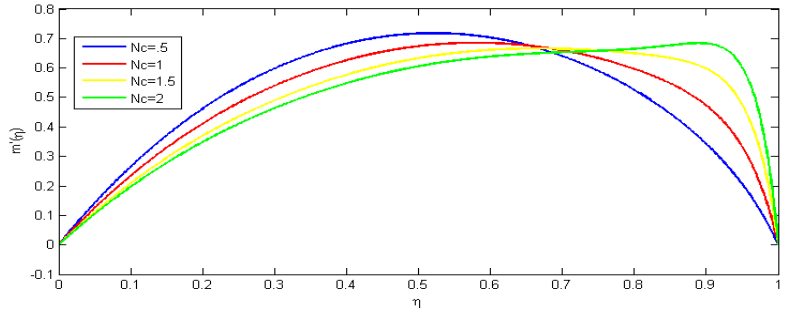

Fig. 6b. Shows the graph of $m'(\eta), m(\eta), n(\eta)$ and $k(\eta)$ with various values of , N_c and constant values of $N_b = 0.1, N_d = .5, N_{em} = 3, P_r = .1, H_m = 10, P_m = 1, P_s = 1, m_\eta = .1, E_c = 0.1$

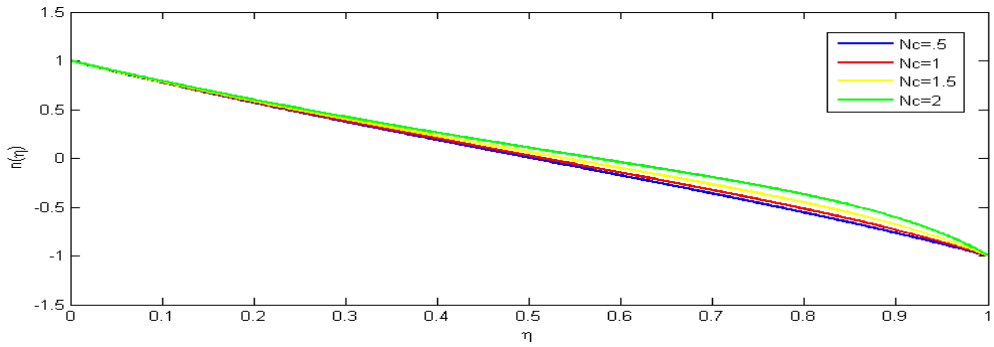

Fig. 6c. Shows the graph of $m'(\eta), m(\eta), n(\eta)$ and $k(\eta)$ with various values of , N_c and constant values of $N_b = 0.1, N_d = .5, N_{em} = 3, P_r = .1, H_m = 10, P_m = 1, P_s = 1, m_\eta = .1, E_c = 0.1, N_c$

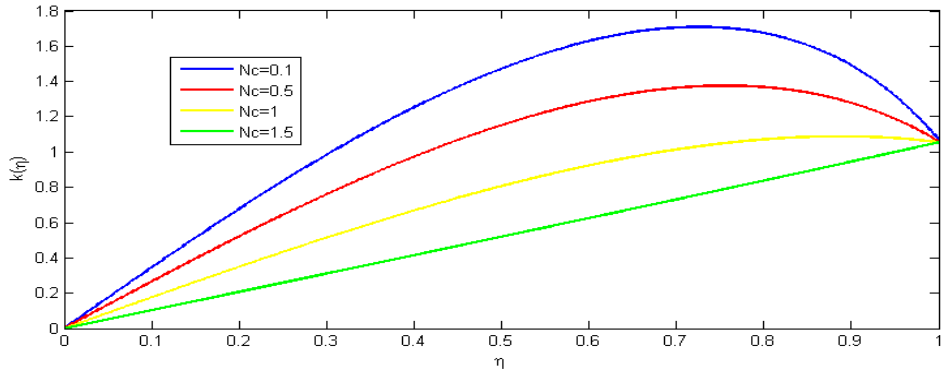

Fig. 6d. Shows the graph of $m'(\eta), m(\eta), n(\eta)$ and $k(\eta)$ with various values of , N_c and constant values of $N_b = 0.1, N_d = .5, N_{em} = 3, P_r = .1, H_m = 10, P_m = 1, P_s = 1, m_\eta = .1, E_c = 0.1,$ $N_c = 3$

Fig. 6 shows the effect of N_c on velocity component in y-direction i.e. $m(\eta)$ and on velocity component in x-direction i.e. $m'(\eta)$. As N_c shows the strength of applied magnetic field in y-direction, so on increasing N_c the velocity component in x-direction i.e. $m'(\eta)$ decreases in the surrounding of lower plate while it increases near the region of upper plate in Fig. 6b. Fig. 6a indicates that as the velocity component in y direction i.e. $m(\eta)$ decreases. Fig. 6 (c-d) shows that on increasing N_c the velocity component in z-direction i.e. $n(\eta)$ near to upper plate are increasing and it decrease the magnetic component in z-direction i.e. $k(\eta)$.

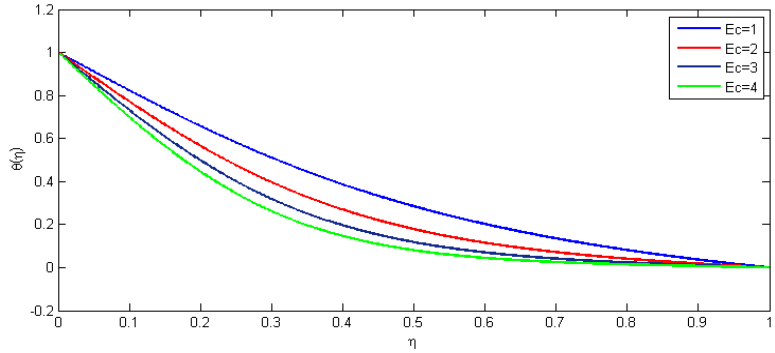

Fig. 7a. Shows the graph of $\theta(\eta), \varphi(\eta)$, with various values 0f E_c and constant values of $N_b = 0.2, N_d = 1, N_{em} = .5, P_r = 10, H_m = 10, P_m = 1, P_s = .5, m_\eta = 2, E_c = 0.1 \quad N_c = 3$

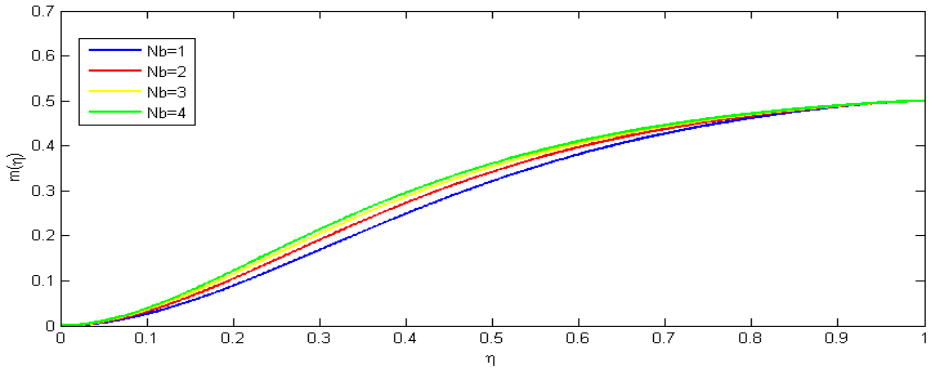

Fig. 8a. Shows $m'(\eta)$, m (η), n(η), k(η), the θ(η)and ϕ(η) with various values ofN_b and constant values of$N_c = 8, N_d = .1, N_{em} = 3, P_r = 2, H_m = 10, P_m = 1, P_s = .5, m_\eta = .1, E_c = 0.1$

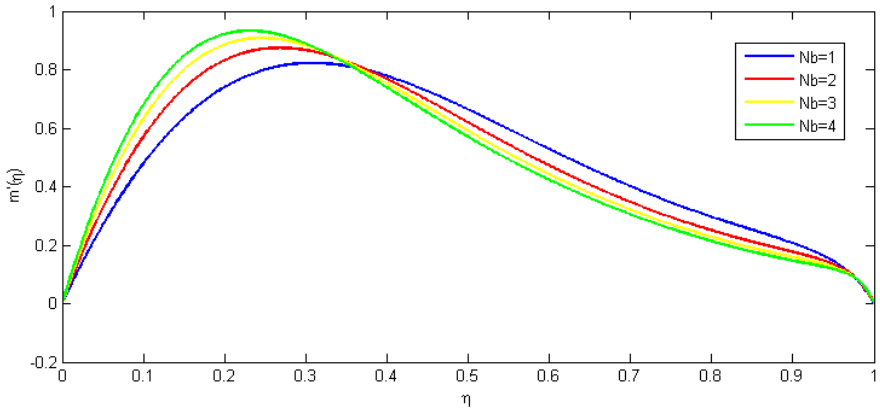

Fig. 8b. Shows $m'(\eta)$, m (η), n(η), k(η), the θ(η)and ϕ(η) with various values ofN_b and constant values of$N_c = 8, N_d = .1, N_{em} = 3, P_r = 2, H_m = 10, P_m = 1, P_s = .5, m_\eta = .1, E_c = 0.1$

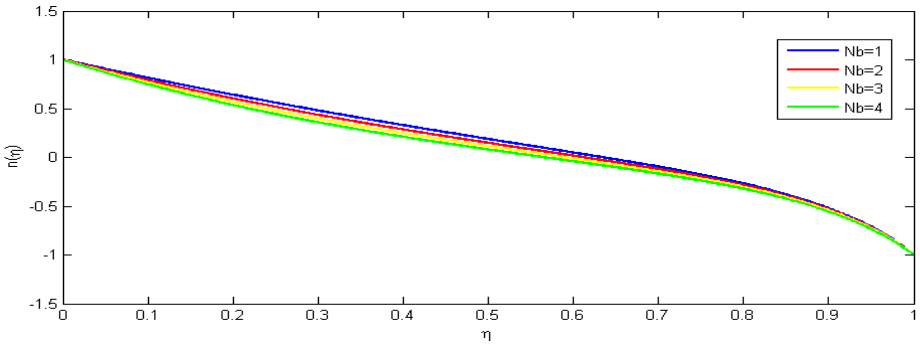

Fig. 8c. Shows $m'(\eta)$, m (η), n(η), k(η), the θ(η)and ϕ(η) with various values ofN_b and constant values of$N_c = 8, N_d = .1, N_{em} = 3, P_r = 2, H_m = 10, P_m = 1, P_s = .5, m_\eta = .1, E_c = 0.1$

The Eckert number E_c is the ratio of the kinetic energy to the boundary layer enthalpy difference and is used to characterized heat dissipation. Fig. 7(a) Shows the increasing E_c decreasing the $\theta(\eta)$, due to temperature difference.

The squeezing Reynold number N_b present the ratio between normal velocity of upper body and kinematic viscosity of the fluid. Fig. 8 shows the effect of squeezing Reynold number on velocity component of $m(\eta) and\ m'(\eta)$. Fig. 8a indicates that as the squeezing Reynold's number increases the velocity component in x-direction decreases in the surrounding of lower plate while it increases near the region of upper plate. Similarly, opposite behavior can be seen in Fig.

3b where the y-component of velocity increases. Fig. 8c indicate that the squeezing Reynold number increase the velocity component in z direction decrease.

Also Table 2 shows increase in viscosity decrease in skin friction $m''(0)$ and slightly increase heat flux $-\theta'(0)$. Similarly, effect of N_{em} andE_c is shown in Tables 3-4. Tables 5-6 shown the effect of P_m and P_s on $m'', n', h', \theta' \; and \; \varphi'$.

4. CONCLUDING REMARK

The mathematical formulation for the constitutive expression, Maxwell equations, energy equation and concentration equation for an unsteady of viscous fluid is employed to model the flow between the two squeezing plates in the form of equations (7) - (12), subject to the boundary conditions given in equation (3.13). Analysis of these equations are performed by PCM and compared with numerical results obtain from BVP4C Package. The following conclusions are drawn with the help of tabulated and graphical results:

- Opposite behavior of the velocity along the x-axis and y-axis with increase in MFD viscosity.
- Magnetic field distribution h(η) decrease with increasing Magnetic Reynold number
- Eckert number have same effect on $\theta(\eta), \psi(\eta)$.
- Opposite behavior of X component and y component of velocity with increasing Squeezing Reynold number
- Table 2. show that $m''(0)$ decrease and increase -θ' with increasing MFD viscosity

COMPETING INTERESTS

Authors have declared that no competing interests exist.

REFERENCES

1. Hathaway DB. Use of ferrofluid in moving-coil loudspeakers. Db-Sound Engineering Magazine. 1979;13(2):42-44.
2. Morimoto Y, Akimoto M, Yotsumoto Y. Dispersion state of protein-stabilized magnetic emulsions. Chemical and pharmaceutical bulletin. 1982;30(8):3024-3027.
3. Soward AM. An Introduction to Magnetohydrodynamics. By PA DAVIDSON. Cambridge University Press, 2001. 431 pp. Journal of Fluid Mechanics. 2002;450:408-410.
4. Rashidi MM, Rostami B, Freidoonimehr N, Abbasbandy S. Free convective heat and mass transfer for MHD fluid flow over a permeable vertical stretching sheet in the presence of the radiation and buoyancy effects. Ain Shams Engineering Journal. 2014;5(3):901-912.
5. Khan A, Shah RA, Shuaib M, Ali A. Fluid dynamics of the magnetic field dependent thermosolutal convection and viscosity between coaxial contracting discs. Results in Physics. 2018;9:923-938.
6. Mutua N. Stokes problem of a convective flow past a vertical infinite plate in a rotating system in presence of variable magnetic field (Doctoral dissertation); 2013.
7. Seth M. The problem considered when the fluid flow is confined to porous boundaries with suction and injection. Langmuir. 2011;29(46):14057-14065.
8. Job VM, Gunakala SR. Unsteady mhd free convection Couette flow between two vertical permeable plates in the presence of thermal radiation using galerkin's finite element method. International Journal of Mechanical Engineering. 2013;2(5):99-110.
9. Simon D. Effect of heat of transfer on unsteady MHD couette flow between two infinite parallel porous plates in an inclined magnetic field. Inter. J. Math. Stat. In. 2014;2(6):2321-4767.
10. Rashidi MM, Freidoonimehr N, Momoniat E, Rostami B. Study of nonlinear MHD tribological squeeze film at generalized magnetic reynolds numbers using DTM. PloS one. 2015;10(8):e0135004.
11. Shrama PR, Singh G. Steady MHD natural convection flow with variable electrical conductivity and heat generation along an isothermal vertical plate. Journal of Applied Science and Engineering. 2010;13(3):235-242.
12. Hunt JC, Holroyd RJ. Applications of laboratory and theoretical MHD duct-flow studies in fusion-reactor technology; 1977.
13. Morley NB, Malang S, Kirillov I. Thermofluid magnetohydrodynamic issues for liquid breeders. Fusion science and technology. 2005;47(3):488-501.
14. Khan A, Shah RA, Shuaib M, Ali A. Fluid dynamics of the magnetic field dependent

thermosolutal convection and viscosity between coaxial contracting discs. Results in Physics. 2018;9:923-938.

15. Aly AM, El-Sapa S. Double rotations of cylinders on thermosolutal convection of a wavy porous medium inside a cavity mobilized by a nanofluid and impacted by a magnetic field. International Journal of Numerical Methods for Heat & Fluid Flow; 2021.

16. Nath R, Murugesan K. Impact of nanoparticle shape on thermo-solutal buoyancy induced lid-driven-cavity with inclined magnetic-field. Propulsion and Power Research. 2022;11(1):97-117.

17. Tijani YO, Oloniiju SD, Kasali KB, Akolade MT. Nonsimilar solution of a boundary layer flow of a Reiner–Philippoff fluid with nonlinear thermal convection. Heat Transfer; 2022.

Peer-review history:
The peer review history for this paper can be accessed here:
https://www.sdiarticle5.com/review-history/88254